GRAIN BOUNDARY STRUCTURE AND DYNAMICS

Douglas L. Medlin, John C. Hamilton and Mark van Schilfgaarde

Technical Highlights

Sandia National Laboratories
Livermore, CA

Term of review FY99 – FY2001

Contact:Robert Q. Hwang,
Sandia National Laboratories, Livermore, CA 94551
Telephone: (925) 294-1570
Fax: (925) 294-3231
Email: rqhwang@sandia.gov

Sandia National Laboratories

GRAIN BOUNDARY STRUCTURE AND DYNAMICS

Douglas L. Medlin, John C. Hamilton and Mark van Schilfgaarde
September, 2001

Table of Contents

OBJECTIVE

Although the importance of grain boundaries in controlling the properties and behavior of polycrystalline materials has long been recognized, many fundamental aspects of grain boundary behavior remain poorly understood [1,2]. Nevertheless, advances in *in situ* and atomic resolution microscopies, and interface computational methods are now bringing us to an exciting time for grain boundary research by providing an unprecedented set of tools for probing the structure and dynamics of these ubiquitous elements of microstructure.

Our program seeks, through a combination of experimental and theoretical studies, to determine the inter-relationships between grain boundary structure and the mechanisms by which grain boundaries move and respond to external forces. This goal is a natural evolution from the earlier years of our program during which we concentrated on determining the static structure of high symmetry boundaries. This early work from our group[3, 4] and others, e.g.[5-7] was

instrumental in developing confidence, and an appreciation of the limits, in the correspondence between experimental observations and theoretical calculations of structure at metallic grain boundaries. However, we are now moving beyond the stage of validating interatomic potentials, to a more complicated class of questions that asks: *What is the physical significance of the boundary structures that we observe and calculate and how is this manifested in the dynamical behavior of the boundaries?*

We feel that the key to establishing this connection is in understanding the behavior of interfacial defects. Just as bulk crystal behavior is dominated by the properties of lattice defects, one anticipates that grain boundary processes are similarly controlled by the properties of the point (e.g., vacancies and impurities) and extended defects (steps, dislocations, and junctions) present on the interface. Formal, crystallographic methods for specifying the geometric character of interfacial steps and dislocation are now well established [8-10], and such methods are now being extended to describe the geometry of boundary junctions [11-13]. What remains an ongoing challenge is to understand the structural relaxations at the cores of such defects and how (or if) these structures can be related across differing interfacial geometries. As we build this framework, we seek ultimately to link this structural information to the factors controlling defect motion, and overall boundary dynamics.

Over the last several years our program has focussed on understanding the structure and behavior of grain boundary dislocations and how these are related to their analogues in the bulk. We have begun to address the behavior of more complicated interfacial defects, such as boundary junctions, and we are now moving towards investigating interfacial point defects. Ultimately, a comprehensive picture of how these seemingly disparate structural elements work in concert will improve our ability to predict and control a diverse range of interface mediated materials processes including slip localization and transmission at boundaries, recrystallization and grain coarsening, grain boundary sliding, and interfacial phase transformations.

APPROACH

We are investigating the structure and dynamical behavior of grain boundaries through a coupled program of experimental and theoretical methods. Our experimental effort utilizes both conventional and high-resolution transmission electron microscopy, to probe the elements of interfacial structure, and *in situ* measurements, to directly investigate the dynamic processes of interfacial motion and dislocation-grain boundary interaction. In our experiments, we investigate systems of carefully controlled crystallographic geometry, fabricated either through bulk bicrystal methods or through thin film epitaxial growth. Our theoretical work combines continuum elasticity, interfacial crystallography, atomistic simulations, and first-principles computations. We are using both semiempirical methods, such as the embedded atom method [14], and newer state-of-the-art first principles and transition state finding techniques [15]. The semiempirical approaches allow rapid qualitative testing of concepts in grain boundary dynamics. For first principles calculations, we are using VASP [16, 17], which allows quantitative calculations of grain boundary properties. For example, we have used VASP and transition state finding to calculate the ideal shear strength of an aluminum Σ=3 {112}boundary [18]. These calculations also reveal the coordinated atomic displacements associated with grain boundary migration coupled to grain boundary sliding. Throughout, our approach is to employ both experimental and theoretical tools to obtain a basic scientific understanding of the fundamental structural elements, interactions and excitations that govern grain boundary behavior.

FACILITIES

Sandia/California is well equipped with analytical instrumentation for conducting our experimental investigations of structure and dynamics. A range of transmission electron microscopes are used in our work. For studies of atomic-scale structure, we employ a 400 kV JEOL 4000EX high resolution TEM (Scherzer resolution 1.7Å). Our *in situ* observations are conducted in a 200 kV JEOL 2010F field emission gun TEM, which is equipped with video-rate cameras and both heating and cooling double-tilt specimen stages. X-ray and electron energy loss spectrometers for chemical microanalysis are also available on this instrument. Finally, we utilize a conventional 120 kV JEOL 1200EX LaB6 TEM. The large tilt range of ±60° on this instrument is important for detailed diffraction contrast studies of dislocations and related defects. In addition to our TEM instrumentation, we have access at this site to full suite of standard microstructural characterization methods including SEM and microprobe, electron backscatter diffraction, and x-ray diffraction.

First principles calculations are computationally intensive as are semiempirical calculations involving huge numbers of atoms or lengthy time scales. In order to carry out such calculations, parallel processing is highly desirable if not essential. The BES program is fortunate in having access to some of the fastest computers in the world. Some of these computers are owned by our group, others are shared with other groups at the Sandia California site, and still others are at other national laboratories and national user facilities. Our group owns two parallel processing machines, including an 8 processor SGI Origin 2000, and a total of 44 DEC alpha processors set up as a cluster for parallel computing. There are also about a dozen single and dual processor workstations owned by the group. At the California site, we use a 64 processor SGI Origin 2000.

The BES materials program is the major (90% access) user of this machine. In addition the California site has a total of 640 DEC alpha processors arranged in clusters for parallel computing. Finally, we have access to extremely powerful machines at Lawrence Livermore Lab, Sandia Albuquerque, and NERSC. Machines which have been used in the BES programs include, but are not limited to, ASCI Red (4510 Intel processors), ASCI White (8194 IBM processors), and two NERSC supercomputers (512 IBM processors and 64 SGI processors).

PERSONNEL

Principal Investigators: John C. Hamilton, Douglas L. Medlin, Mark van Schilfgaarde

Post-doctoral and Limited Term Researchers:

Cindy Kelchner: August 1996- June 1998
Babak Sadigh: January 1998-July 1998
Oleg Mryasov: September 1999-August 2001
Istvan Daruka: October 1999-present
Dov Cohen: May 1999 to January 2000
Gene Lucadamo: June 2000-Present
Don Siegel: September 2001-Present
Sergey Faleev: September 2001-Present
Derek Steward: September 2001-Present

COLLABORATIONS

C.B. Carter, University of Minnesota. We have had a long-standing collaboration investing dislocation models for grain boundary structure.

C.L. Briant, Brown University: We are working with Brown University to investigate the structure of near Σ=9 boundary in Aluminum in order to better understand the role of interfacial dislocations at this boundary.

G.H. Campbell, LLNL. We collaborated with LLNL to investigate the dislocation processes involved in the dissociation of a copper Σ=3 grain boundary.

E. Stach, LBL-NCEM. In our planned work, we will be utilizing the new *in situ* high resolution transmission electron microscope at the user facility of the LBL National Center for Electron Microscopy.

S.M. Foiles, SNL/NM We have continued collaborations on theoretical calculations of grain boundary structure.

PROFESSIONAL AWARDS AND SERVICE

(Medlin) Organizer: symposium on "Influences of Interface and Dislocation Behavior on Microstructure Evolution" held at the Fall 2000 Meeting of the Materials Research Society.

(Medlin) Member (since 1999), International Advisory Committee for the *Intergranular and Interphase Boundaries in Materials* conference series.

(Medlin) Council Member (since 2000) Northern California Society for Microscopy.

(Medlin) Organizer: symposium on "Thin Film Microstructure Analysis" to be held at the Scanning 2002 meeting, May, 2002.

PUBLICATION LIST

"Dislocation Nucleation and Defect Structure During Surface Indentation," C. L. Kelchner, S. J. Plimpton, and J. C. Hamilton, *Physical Review B* 58, 11085 (1998).

"Effect of Surface Steps on the Plastic Threshold in Nanoindentation" J.D. Kiely, R.Q. Hwang, J.E. Houston, Physical Review Letters 81 (20) (1998) 4424-4427.

“Stacking Defects in the 9R Phase at an Incoherent Twin Boundary in Copper,”
D.L. Medlin, G.H. Campbell, and C. B. Carter, *Acta Materialia* 46 (14) (1998) 5135.

“Effect of Grain Boundary Dislocations on 9R Stacking Errors at an Incoherent Twin Boundary in Copper” D.L. Medlin, S.M. Foiles, G.H. Campbell, C.B. Carter, *Materials Science Forum* 294-298 (1999) 35-42 (Invited).

"Observation and Modeling of $\frac{1}{3}$ <111 > Twin Dislocations in Aluminum,"
D.L. Medlin, in: Advances in Twinning. eds. S. Ankem and C.S. Pande (TMS, 1999) 29-40. (Invited)

"Morphological Evolution of a Fully Faceted Grain Boundary," D.L. Medlin and G. Lucadamo, in "Influences of Interface and Dislocation Behavior on Microstructure Evolution," eds. M. Aindow *et al.* (2001, MRS).

“New features of dislocation structures arising from lattice discreteness,”
O.N. Mryasov, Y.N. Gornostyrev, and A.J. Freeman, see LANL cond-mat/0006257 (2000) (unpublished)

“Complex Evolution of Dislocation Core Structure in a Process of Motion: Model Analysis with *ab initio* Parameterization,” O. Mryasov, Y.N. Gornosryev, M. van Schilfgaarde and A.J. Freeman, Mat Sci. and Engineering A309, 310 (2001).

“A Dislocation-Based Description of Grain Boundary Dissociation: Application to a 90 Degree <110> Tilt Boundary in Gold” D.L. Medlin, S.M. Foiles, and D. Cohen, *Acta materialia*. **49** (18) 3687-3695 (2001)

"Surface Step Effects on Nanoindentation", J. A. Zimmerman, C.L. Kelchner, P.A. Klein, J.C. Hamilton, S.M. Foiles, accepted for publication in Physical Review Letters. (2001). To appear October 15, 2001.

"Structure and Climb of $\frac{1}{3}$ <111> Twin Dislocations in Aluminum" S.M. Foiles and D.L. Medlin, accepted for publication in *Materials Science and Engineering A* (2001).

"Dislocation Emission around Nanoindentations on a (001) fcc Metal Surface Studied by STM and Atomistic Simulations", O. Rodriguez de la Fuente, J. A. Zimmerman, M. A. Gonzalez, J. de la Figuera, J. C. Hamilton, W.W. Pai, J.M. Rojo, Submitted to Physical Review Letters

"First-Principles Calculations of Grain Boundary Theoretical Shear Strength Using Transition State Finding to Determine Generalized Gamma Surface Cross Sections",
J. C. Hamilton and S.M. Foiles, submitted to *Physical Review B* (2001).

“Dislocation Emission at Junctions between Σ=3 Grain Boundaries in Gold Thin Films” G. Lucadamo and D.L. Medlin, submitted to *Acta materialia* (2001)

"Grain Boundary De-faceting: A first order phase transition by atomic shuffle", I Daruka and J.C. Hamilton, to be submitted.

Invited Conference Presentions

J. C. Hamilton, Istvan Daruka, "Grain Boundary De-faceting: a First Order Phase Transition by Atomic Shuffle", presented at the Fall Meeting of the Materials Research Society, Boston, MA, December 1, 2000.

D.L. Medlin, "Structure and Dynamics of Grain Boundary Defects" presented at the TMS Annual Meeting, Symposium on High Resolution Electron Microscopy in Materials Science, Nashville TN, March 12-16, 2000.

D.L. Medlin, "Observation and Modeling of Grain Boundary Dislocation Structure and Behavior, " presented at the TMS Annual Meeting, Symposium on Dislocations and Microscale Plasticity Modeling, Nashville TN, March 12-16, 2000.

D.L. Medlin, "Interfacial Dislocation Structure and Dynamics at Incoherent Twin Boundaries" presented at the "International Symposium on Advances in Twinning" at the TMS Annual Meeting, San Diego CA, February 28 - March 4, 1999.

D.L. Medlin, "Electron Microscopy Analysis of Microstructure at Metal and Metal-Ceramic Interfaces" Golden Gate Materials and Welding Technologies Conference, San Francisco, CA, February 4-5, 1999.

D.L. Medlin, “Defect Structures at Incoherent Twin Boundaries” presented at the 9th International Conference on Intergranular and Interphase Boundaries in Materials, Prague, Czech Republic, July 6-9, 1998.

SUMMARY OF ACCOMPLISHMENTS

At an atomic level, grain boundaries are highly complex systems. Our approach is to identify the relevant and hopefully fewer mechanisms that govern their motion and evolution. By linking experimental observations with simulations on a range of length scales, we strive to identify these mechanisms and use them to build generic models of grain boundary dynamics.

Our work on dislocation core structures has led to improved descriptions of dislocation dissociation, addressed the processes of dislocation nucleation at surfaces, and provided insight into the mechanisms of interfacial dislocation motion. Our theoretical investigations have produced greatly improved methods for visualizing and analyzing lattice and grain boundary defects in large-scale atomistic simulations. First principles calculations have allowed us to calculate the theoretical shear strength of a grain boundary. Our studies of interfacial structure, in particular analyses of dissociated boundaries, are pointing to the important role of Shockley partial type dislocations as fundamental elements of interfacial structure--an important step in developing a unified picture of the dependence of grain boundary structure on orientation. Finally, our theoretical analysis of facet junction core structure has identified the elementary excitations involved in grain boundary defaceting phase transitions. Through experimental measurements, we are now probing how boundary junctions interact with each other and with other interfacial defects during grain evolution.

Extended Peierls-Nabarro Model

(References [19, 20]) See publications collection.

Dislocations are complex defects to study from first principles because they require description both at atomic scale in the vicinity of the core, but also at the mesoscopic scale, owing to the long-ranged strain fields [21]. In this work we start from the Peierls-Nabarro model, but extend it to a completely atomistic theory that eliminates some of the key inconsistencies of the original model [22]. By parameterizing the misfit energy in terms of the so-called γ-surface [23], which is computed within the *ab initio* Local-Density Approximation [24], the approach is free of empirical or adjustable parameters. A model results which is fully two-dimensional, accurate and predictive; and compact, spread, and split dislocations are unified into a single description. New features of dislocations were found, including the possible existence of multiple dislocation core structures arising from the non-continuum nature of the core. As an illustration of the principle, the effects of the lattice and multiple core structures was investigated for CuAu under different stress conditions.

Observation and Modeling of the Core Structure of Dissociated $\frac{1}{3}$ < 111 > Twin Dislocations

(References [25, 26]) See publications collection.

The dynamic behavior of interfaces is controlled in part by the properties of interfacial defects. We have combined atomistic modeling and HRTEM imaging to determine the core structure of $\frac{1}{3}$ <111 > twin dislocations in aluminum. Analysis of the atomic configuration of these defects shows that they possess a dissociated core. The structural details can be understood as the decomposition of the defect into a Shockley partial dislocation, which is emitted from the

interface, and a stair-rod dislocation, which remains in the interface plane. These results provide insight into a new mechanism of twin growth involving dislocation*climb* rather than *glide*.

Aluminum Grain Boundary Sliding

(Reference [18]) See publications collection.

Grain boundary sliding plays a major role in the stress induced deformation of polycrystalline materials at high temperatures. We have used first-principles nudged-elastic-band calculations to understand grain boundary sliding at the Al$\Sigma 3(11\bar{2})$ incoherent twin boundary. We find that the theoretical shear strength of this grain boundary is an order of magnitude smaller than that of single crystal aluminum [27]. We also show the atomic mechanism responsible for grain boundary migration during sliding. An important conclusion is that the usual definition of the γ-surface for a grain boundary must be changed in order to allow for cooperative atomic motions at the grain boundary which occur during sliding and at the core of grain boundary dislocations. A movie illustrating the atomic rearrangments accompanying the grain boundary sliding is included on the accompanying CD-ROM.

(Filename: **al grain boundary sliding**).

Influence of Dislocation Structure on the 9R Reconstruction at Σ=3 Grain Boundaries

(References: [28, 29]) See publications collection.

Dissociation of grain boundaries into three-dimensional configurations is now known to be a wide-spread and important mode of interfacial relaxation [30-33]. However, the factors controlling the atomic structure of the intermediate layer have been unclear. The prototypical example of this effect is the reconstruction of FCC Σ=3 {112} boundaries in low stacking fault energy metals to form a nanometer-scale layer with 9R stacking[34, 35]. This arrangement is equivalent to inserting a stacking fault every third close-packed plane. Our experimental and theoretical analysis of perturbations in the 9R stacking in a dissociated Σ=3 boundary in copper has shown that the structure is directly related to the specific set of Shockley partial dislocations that comprise the interface. This suggests a new description of grain boundary structure as stacking sequences of partial dislocations.

Dislocation-Based Model for Grain Boundary Dissociation

(Reference: [36]) See publications collection.

Our previous success describing boundaries near the Σ=3 orientation as arrays of Shockley partial dislocations has motivated us to investigate whether such an approach can be generalized to treat boundaries of greater complexity. We have shown that by partitioning the grain orientation into two components--a “twinning” rotation, produced by the operation of an array of Shockleys, and a “shape change,” arising from the net Burgers vector of the array--it is possible to predict the specific set of Shockley partial dislocations that comprise an interface. We have applied this model to explain the experimental observations of a dissociated 90°{111}/{112} boundary in Au. By successfully describing the decomposition mode and geometrical features of this interface, our work demonstrates the importance of Shockley partial dislocations as elements of interfacial structure and provides a key step in testing whether general high angle grain boundaries can be understood in terms of arrays of such defects.

Multi-Scale Modeling of Grain Boundary De-faceting Phase Transition

(Reference: [37]) See publications collection.
Phase transitions are a fundamental process in chemical physics, yet until recently our understanding of phase transitions at grain boundaries has been extremely limited. A seminal paper by Cahn [38] presents a thermodynamic discussion of transitions and phase equilibria among grain boundary structures. Perhaps the best-documented grain-boundary phase-transition is the experimental observation of the reversible de-faceting of a Σ=3 Al grain boundary with an average $[1\bar{1}0]$ orientation [39]. At temperatures below about 400K the grain boundary consists of large $[11\bar{2}]$ facets. At higher temperature the facets disappear. We have formulated a complete atomistic and lattice model of this phase transition. The elementary excitation responsible for the phase transition is defined based on atomistic simulations of the grain boundary. This elementary excitation is mapped onto a two-dimensional lattice model. The phase transition in the 2D lattice model is investigated by Monte Carlo simulations and by analytical statistical mechanics. This 2D lattice model exhibits a first order phase transition, in dramatic contrast to surface roughening phase transitions. A movie showing this defaceting phase transition is included on the accompanying CD-ROM. (Filename: **al grain boundary defaceting**)

Morphological Evolution of Grain Boundary Facets
(Reference: [40]) See publications collection.
We are conducting experiments to better understand the behavior of grain boundary facets junctions during microstructural evolution in Au thin films. From these observations, we have learned that facet coarsening is accompanied by the motion of perimeter conserving facets (*i.e.*, facets terminated by corners of opposite sense with respect to the Wulff surface). Our observations are surprising in light of the conventional view of grain-boundary facet evolution. Perimeter conserving facets have been thought to remain fixed until being passively consumed by facets terminated by corners of the same sense (which do not conserve the boundary perimeter and thus lead to a net reduction in interfacial energy) [41]. Thus an important question is raised: are there energetics associated with the junctions themselves that produce a driving force for facet motion? To address this question, we are currently measuring the short-time fluctuations in junction position to determine whether correlations exist that would be indicative of junction-junction interactions. A movie showing an example of the facet evolution is provided on the accompanying CD-ROM.
(Filename: **grain boundary facet evolution**)

Origin of Dislocations at Grain Boundary Facet Junctions
(Reference: [42]) See publications collection.
Dislocation arrays that appear to emanate from grain boundary junctions are commonly observed in thin films [43-45]. Since such dislocations can play important roles in both the microstructural evolution and strain response of a thin film, it of interest to determine their origin and relationship to grain boundaries. Using *in situ* TEM, we have investigated the behavior of dislocations at grain boundary facet junctions in [111] oriented gold films. Our results show a simple process by which grain boundary dislocations can be transformed to a glissile configuration at a twin boundary. This work identifies a strain relief mechanism that should be considered in analyses of plasticity in polycrystalline thin films. A movie showing an example of dislocation motion past a grain boundary facet junction is provided on the accompanying CD-ROM.

Atomistic Models of Dislocation Nucleation during Nanoindentation

(References: [46-49]) See publications collection.

This work used the embedded atom method to model surface indentation of gold surfaces by a tip with a radius one order of magnitude smaller than an experimental atomic force microscope tip. The indentation was performed quasi-statically, and force curves were plotted as a function of tip displacement. A key accomplishment was the development of the "centrosymmetry parameter" which allows the location of lattice defects to be pin pointed given a list of atomic positions. This parameter allows imaging and differentiation of partial dislocations and stacking faults produced by surface indentation. This allows specific dislocation nucleation events to be correlated with force vs. displacement curves, providing insight into the experimental indentation process. Movies showing atomistic simulations of the dislocation nucleation during indentation and the dislocation structure after indentation are included on the accompanying CD-ROM.

(Filenames: **au111 indentation nucleation** and **au111 indentation rotation**)

TECHNICAL HIGHLIGHTS

Extended Peierls-Nabarro Model

Mark van Schilfgaarde and O. Mryasov

Publication:

"Complex Evolution of Dislocation Core Structure in a Process of Motion: Model Analysis with *ab initio* Parameterization," O. Mryasov, Y.N. Gornosryev, M. van Schilfgaarde and A.J. Freeman, Mat Sci. and Engineering A309, 310 (2001).

O. N. Mryasov, Y. N. Gornostyrev, and A. J. Freeman, "New features of dislocation structures arising from lattice discreteness," see LANL cond-mat/0006257 (unpublished).

Motivation:

Dislocations are one of the most complex defects to study in a rigorous way because they require a quantum-mechanical description both at atomic scale in the vicinity of the core, but also at the mesoscopic scale, owing to the long-ranged strain fields. Our current understanding of the dislocation motion over the periodic (Peierls) potential is based on the concept of kink formation and migration processes. It has been studied most extensively in the context of the dislocation motion in covalent materials with a large Peierls barrier. In systems such as fcc metals with much smaller Peierls barriers, kinks often play a less important role; there dislocation dynamics of cross-slip, dislocation-point defect interactions and similar processes are the dominant mechanisms. Despite the complexity of these "elementary" dislocation dynamics processes, it is now established within model analyses that they are essentially characterized by a few parameters such as the Peierls barrier for kink processes or partials recombination energy for the cross-slip and these fundamental parameters are strongly dependent on the atomistic features of individual dislocation core structures. They interact with the periodic Peierls potential owing to the lattice discreteness, periodicity and symmetry.

Accomplishment:

The Peierls-Nabarro (PN) model has been essential in elucidating a basic understanding of the relation between lattice geometry, interatomic interactions and dislocation structure. In this work we incorporate atomistic extensions of the PN model resulting in an elegant and powerful approach that eliminates some of the key inconsistencies of the original model. By parameterizing the misfit energy in terms of the so-called γ-surface, which is computed within the *ab initio* LDA, the approach is free of empirical or adjustable parameters. The model is fully two-dimensional, and compact, spread, and split dislocations are unified into a single description. Thus, it is intermediate in rigor between the classical model and a comprehensive approach.. New features of dislocations were uncovered, including the prediction of multiple dislocation core structures and the effects they have on the evolution of a core under stress.

Significance:

This work led to the prediction of new features fundamental to the properties of dislocations.

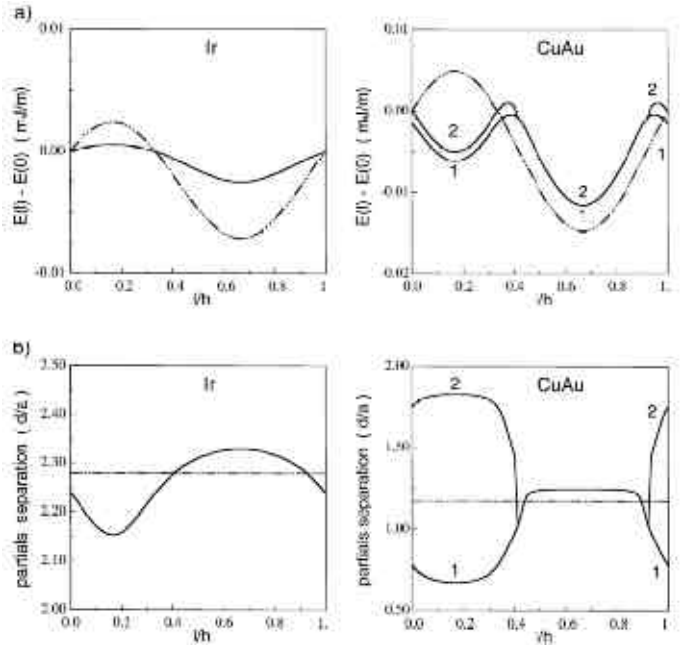

Dislocation energy (a) in *J/m,* and (b) partials separation *d* as functions of the dislocation axis *l.* Computations were made by minimizing the PN total energy while constraining *l.* Results are shown for the ordinary screw dislocations for Ir (left panel) and CuAu (right panel) with a discrete representation (solid lines) and "continuum" representation (dotted-dashed lines) of the misfit energy. Multiple dislocation core structures are manifest by multiple minima in E as a function of l . The equilibrium core structure corresponds to the global minimum. As the lattice is sheared, the relative energies of two minima can reverse, leading to a discontinuous change in the core structure with stress.

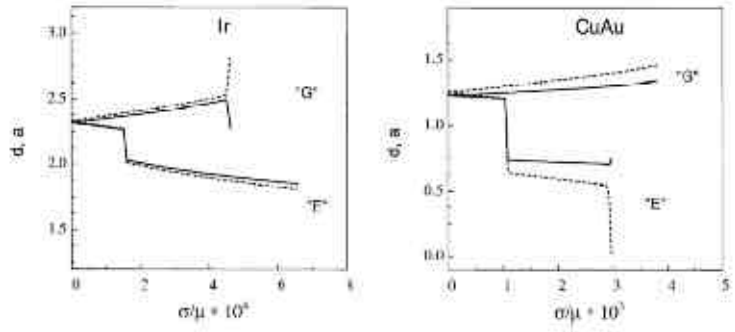

Partials separation d calculated for screw (dashed lines) and edge components (solid lines) of the displacement field of the ordinary dislocation as a function of glide ('G') and Escaig ('E') stresses σ_ (in units of μ, the shear modulus) for fcc Ir and Ll0 CuAu.

Observation and Modeling of the Core Structure of Dissociated $\frac{1}{3}$ < 111 > Twin Dislocations

D.L. Medlin and S.M. Foiles

Publications:

Observation and Modeling of $\frac{1}{3}$ <111> Twin Dislocations in Aluminum, D.L. Medlin, in: Advances in Twinning. eds. S. Ankem and C.S. Pande (TMS, 1999) 29-40. (Invited)

"Structure and Climb of $\frac{1}{3}$ <111> Twin Dislocations in Aluminum" S.M. Foiles and D.L. Medlin, to be published in *Materials Science and Engineering A* (2001).

Motivation:

The dynamic behavior of interfaces is controlled in part by the properties of interfacial defects. In earlier work, we discovered a mechanism by which *climb* of $\frac{1}{3}$ <111> interfacial dislocations can lead to twin growth in FCC materials [D.L. Medlin *et al.*, Phil. Mag. A 75 (3) (1997) 733-747]. This mechanism is distinct from conventional twinning, which occurs by *glide* of 1/6<112> dislocations. Until now, however, the core structure of these interfacial dislocations has been poorly understood.

Accomplishment:

We have combined atomistic modeling and HRTEM imaging to determine the core structure for $\frac{1}{3}$ <111> twin dislocations in aluminum. Figure 1 shows the atomic positions for this defect as predicted using the Embedded Atom Method. In Figure 2, the intensity peak positions from an HRTEM image simulation for the calculated structure are overlaid on the experimentally observed lattice image of this dislocation. Both the calculation and observation show that the dislocation is dissociated. As indicated by the dashed lines on Figures 1 and 2, the center of the dislocation core is positioned away from the {111} twin interface by a distance of about three {111} planes. This atomic configuration can be understood in terms of a classical dislocation dissociation reaction. As is illustrated in Figure 3, the perfect $\frac{1}{3}[\bar{1}\,\bar{1}\,\bar{1}]$ twin dislocation ($\delta\mathbf{D}$ in Thompson's notation) may dissociate by emitting from the interface a Shockley partial dislocation ($\mathbf{b}=\frac{1}{6}[\bar{2}\,\bar{1}\,\bar{1}] = \beta\mathbf{D}$) onto the $(1\bar{1}\,\bar{1})$ plane (which is inclined with respect to the (111) twinning plane). This produces a short segment of stacking fault on the $(1\bar{1}\,\bar{1})$ plane and leaves behind a stair-rod dislocation ($\mathbf{b} = \frac{1}{6}[0\bar{1}\,\bar{1}] = \delta\beta$) at the twin step.

Significance:

The presence of a dissociated core raises an interesting question: must the defect constrict to a compact configuration before absorbing a vacancy and climbing or can the absorption occur along the extended defect? Our calculations show a strong energetic preference for vacancy clustering at the stair rod core and that the dislocation can advance through a double-kink mechanism without needing to constrict. These insights into the detailed behavior at the dislocation core are helping to provide an atomic scale basis for understanding interfacial motion induced by dislocation climb.

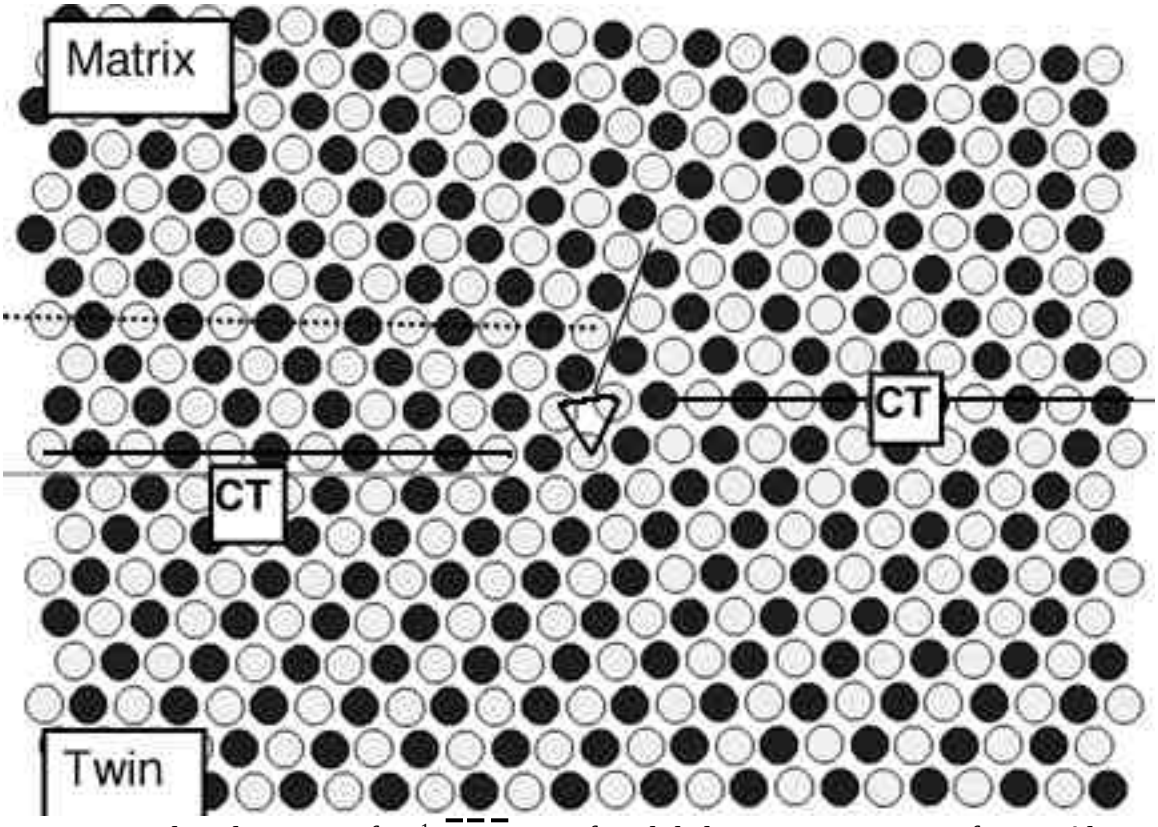

Figure 1: Relaxed structure for $\frac{1}{3}[\bar{1}\,\bar{1}\,\bar{1}]$ interfacial dislocation at twin interface in Aluminum.

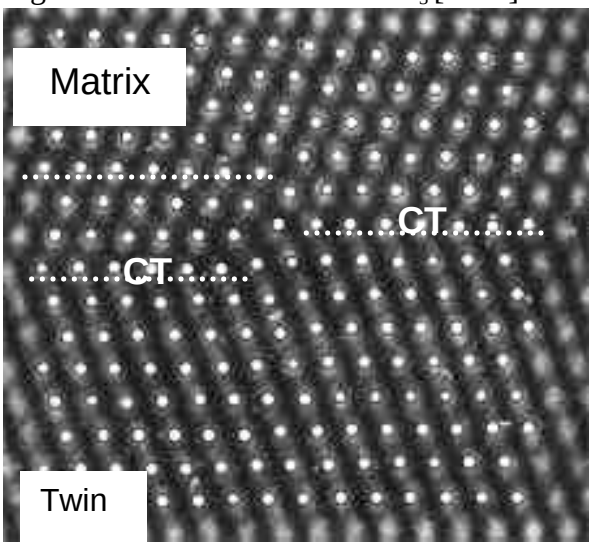

Figure 2: Comparison of calculated structure for twin defect with experimental HRTEM observation. The circles are peak positions from an HRTEM image simulation.

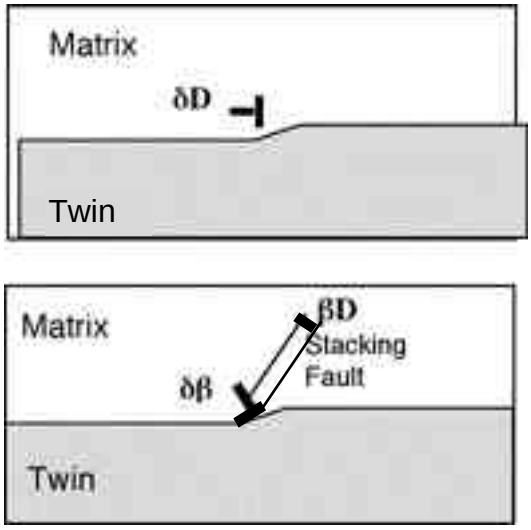

Figure 3. Schematic illustrating dissociation of $\frac{1}{3}[\bar{1}\,\bar{1}\,\bar{1}]$ (δ**D**) dislocation into a stair-rod dislocation (**b** = $\frac{1}{6}[0\bar{1}\,\bar{1}]$ = δβ) and a Shockley partial (**b**=$\frac{1}{6}[\bar{2}\,\bar{1}\,\bar{1}]$ = β**D**) dislocation.

Aluminum Grain Boundary Sliding

J. C. Hamilton and S.M. Foiles

Publication:

"First-Principles Calculations of Grain Boundary Theoretical Shear Strength Using Transition State Finding to Determine Generalized Gamma Surface Cross Sections", J. C. Hamilton and S.M. Foiles submitted to Physical Review B.

Motivation:

In the past we have pursued extensive experimental and theoretical investigations of grain boundaries. These studies have resulted in a detailed understanding of the static structure of aluminum grain boundaries. We are now extending our theoretical studies to include dynamic processes at grain boundaries, including grain boundary sliding. Grain boundary sliding is a complex process which dominates the deformation of polycrystalline metal samples at high temperatures (greater that 4/10 of the melting point).

Accomplishment:

We have used first principles nudged elastic band calculations to calculate the theoretical shear stress of the Aluminum $\Sigma 3$ $[11\bar{2}]$ incoherent twin boundary. This is a commonly occurring low energy grain boundary. It has two different stable configurations as shown in figures 1a and 1c. The stable configurations both have the {111} planes on one side of the grain boundary offset by about 0.7Å relative to the planes on the other side of the grain boundary. Figure 1b shows a symmetric configuration which is the intermediate in shearing from a to c. Further shearing from configuration c eventually produces the stable configuration shown in Figure 1e. This configuration is equivalent to configuration a. Figure 1d shows an antisymmetric configuration which is the intermediate in shearing from c to e. The energy barrier associated with this shear is quite small, only about 10% of the energy required to shear bulk Aluminum along the facile {111} shear planes.

Significance:

This calculation provides fundamental insight into the process of grain boundary shear. We find that the theoretical shear strength of this grain boundary is ten times smaller than the theoretical shear strength of bulk aluminum along the favored slip directions. This accounts for the major role which grain boundary diffusion can play in deformation of polycrystalline samples. We also note that the grain boundary translates in a direction perpendicular to itself as it undergoes shear. This is phenomena has been seen experimentally in Zinc tilt boundaries. Our calculations demonstrate the precise atomic mechanism of this grain boundary translation during shear. We anticipate that the first principles results provided here will be useful in quantitative modeling of the structure of grain boundary partial dislocations at this grain boundary.

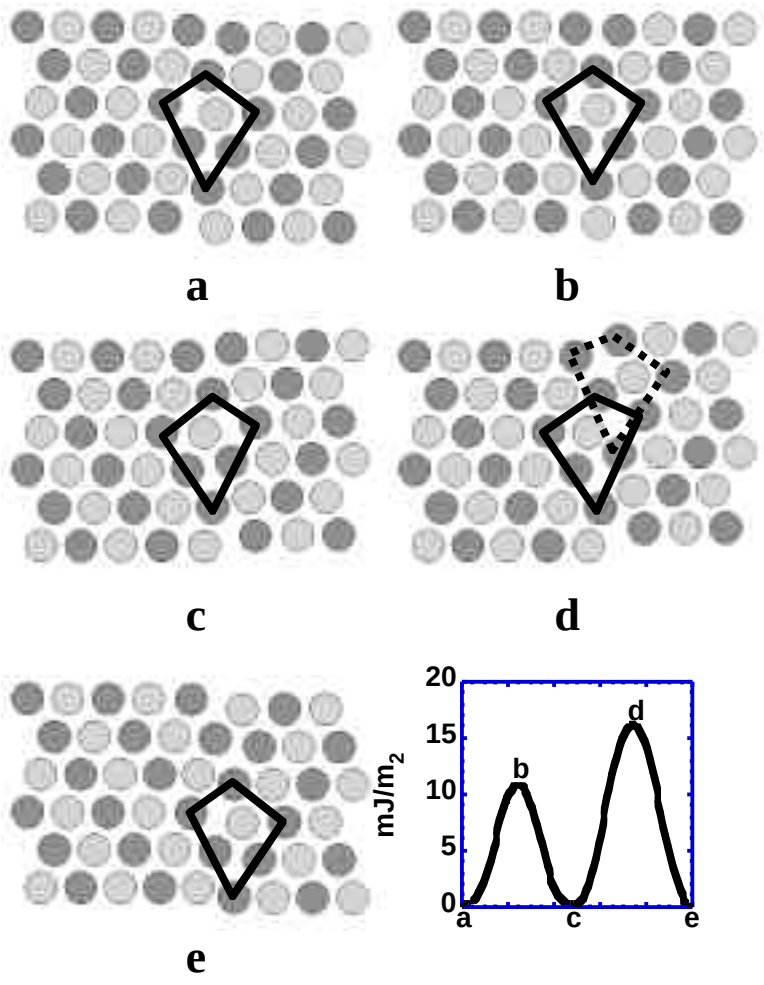

FIGURE 1: Structure and energy of Al $\sum 3$ $[11\bar{2}]$ grain boundary during shear. In (a), a stable configuration of the grain boundary is shown. The lattice on the right hand side of the boundary is offset downward by about 0.7Å relative to the lattice on the left hand side of the boundary. In (b) the lattice on the right hand side of the grain boundary is displaced upward to match the lattice on the left hand side of the grain boundary. We call this the symmetric configuration. In (c) the lattice on the right hand side of the grain boundary is displaced further upward to reach a stable configuration which is related by a symmetry operation to the starting configuration in (a). In (d) the lattice on the right hand side of the grain boundary is displaced upward to reach a configuration with the right hand lattice planes half-way between the left hand lattice planes. We call this the anti-symmetric configuration. In (e) the right hand lattice has been displaced upward again and is now in a stable configuration with the same offset shown in (a). The grain boundary has moved to the right as a result of the sliding. The energy of these configurations determined by a nudged elastic band calculation is shown in the final graph. A movie of the grain boundary sliding and migration is included on the accompanying CDROM (filename: **al grain boundary shearing**).

Influence of Dislocation Structure on the 9R Reconstruction at Σ=3 Grain Boundaries

D.L. Medlin, G. Campbell (LLNL), C.B. Carter (Univ. Minnesota)

Publications:

"Stacking Defects in the 9R Phase at an Incoherent Twin Boundary in Copper," D.L. Medlin, G.H. Campbell, and C. B. Carter, *Acta Materialia* 46 (14) (1998) 5135.

"Effect of Grain Boundary Dislocations on 9R Stacking Errors at an Incoherent Twin Boundary in Copper" D.L. Medlin, S.M. Foiles, G.H. Campbell, C.B. Carter, *Materials Science Forum* 294-298 (1999) 35-42 (invited).

Motivation:

Dissociation of grain boundaries into three-dimensional configurations is now known to be a wide-spread and important mode of interfacial relaxation. However, the factors controlling the structure of the intermediate layer have been unclear. The prototypical example of such dissociation is the FCC Σ=3 {112} boundary. In low stacking fault energy metals, such as copper and silver, this boundary reconstructs into a nanometer-scale layer composed of the 9R phase, a stacking sequence that is related to FCC by the introduction of a stacking fault every third plane. In earlier work, we have shown that the ideal Σ=3{112} boundary can be described by an array of 1/6<112> type dislocations arranged in a repeating sequence of one pure-edge 90° dislocation (**A**δ) and two 30° dislocations (**B**δ + **C**δ). The 9R sequence arises if the 90° and 30° arrays separate and thus the dissociation width can be sensitive to the local strain. In the present work we consider how perturbations in the 9R stacking are related to the dislocation structure of the interface.

Accomplishment:

Figure 1 shows an HRTEM image of a copper Σ=3 boundary that has dissociated into a ~30Å wide layer. Although most of the boundary is in the 9R arrangement, some errors in this sequence can be identified (*i.e.* the 4- and 5-layer faults indicated on the figure). Defect circuit analysis shows that these layers are associated with secondary grain boundary dislocations with Burgers vector type 1/6<112>. The specific fault type can be explained by considering both the sense (positive or negative) and character (pure edge (90°) or mixed (30°)) of the secondary grain boundary dislocation's Burgers vector. For instance, as shown in Figure 2, addition of a single positive 30° dislocation (**B**δ) to the interfacial dislocation sequence increases the spacing between the pure edge, **A**δ, dislocations by one plane, producing a four-plane fault upon boundary decomposition. Similarly, removal of a pure edge (**A**δ) dislocation, which is vectorially equivalent to adding two 30° dislocations (**B**δ +**C**δ), produces a 5-plane fault (Figure 3).

Significance:

These results show the linkage between dislocation content and atomic structure at dissociated grain boundaries. In essence, the dissociated structure is directly related the specific set of Shockley partial dislocations that comprise the interface. This suggests a new description of grain boundary structure in terms of stacking sequences of *dislocations*.

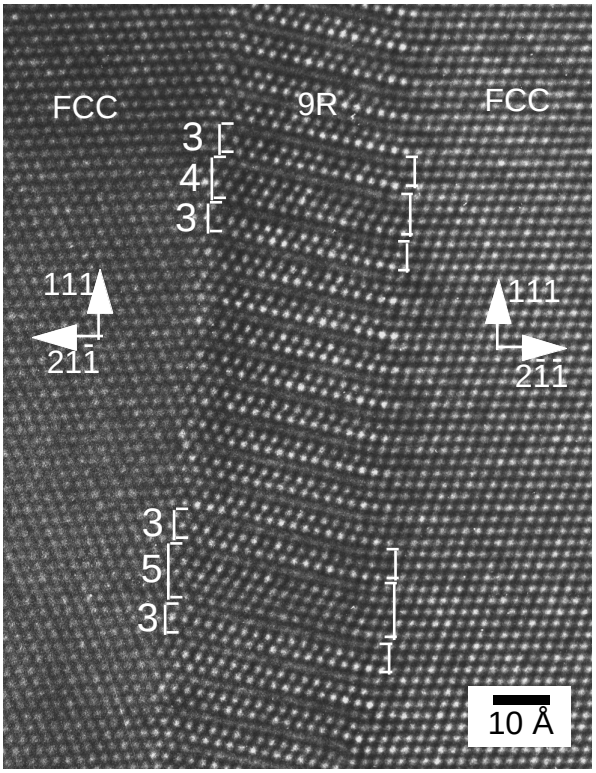

Figure 1. HRTEM image showing 9R region at dissociated Cu incoherent twin boundary. 4- and 5-layer faults in the 9R stacking are indicated.

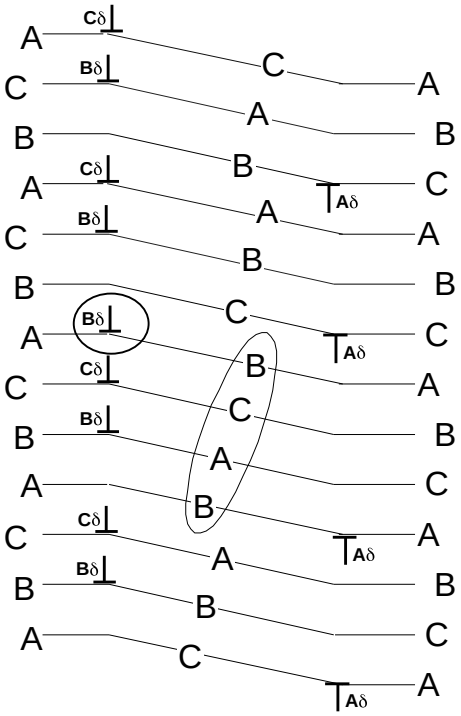

Figure 2. Schematic showing the formation of a 4-layer fault in the 9R layer by insertion of a positive 30° dislocation (**B**δ).

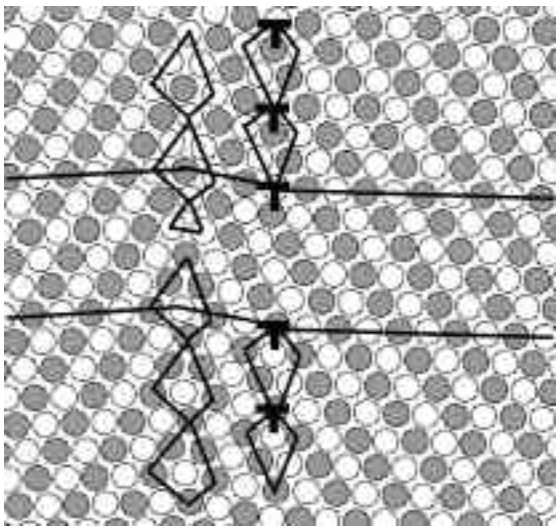

Figure 3. Atomistic calculation (EAM) showing the result of removing a 90° (**A**δ) dislocation from the boundary. Note the 5-layer break in the normal 3-plane periodicity of the interface.

Dislocation-Based Model for Grain Boundary Dissociation

Publication:
"A Dislocation-Based Description of Grain Boundary Dissociation: Application to a 90 Degree <110> Tilt Boundary in Gold" D.L. Medlin, S.M. Foiles, and D. Cohen, *Acta Materialia*. 49 (18) 3687-3695.

Motivation:

Our previous success describing the dissociation of boundaries near the Σ=3 orientation in terms of arrays of Shockley partial dislocations has motivated us to investigate whether such an approach can be generalized to treat boundaries of greater complexity.

Accomplishment:

As illustrated schematically in Figure 1, our approach is to partition the grain orientation into two components: a "twinning" rotation, produced by the operation of an array of Shockleys, and a "shape change," arising from the net Burgers vector of the array. From these considerations it is possible to predict the specific set of Shockley partial dislocations that comprise the interface. We have applied this approach to understand the structure of a 90°{111}/{112} boundary in Au. Figure 1 shows an HRTEM image of this boundary in gold. Examination of the interfacial region shows a narrow stacking fault at every third plane (indicated by the white lines). This fault arrangement is similar to the 9R reconstruction that is observed at Σ=3 {112}boundaries. In the Σ=3 case, the grain orientation and boundary structure are well represented by an array of negative 90° (**A**δ) and positive 30° (**B**δ and **C**δ) Shockley partial dislocations distributed on adjacent {111} planes in a ratio of n_{90}:n_{30}=1:2 (specifically, a repeating sequence: ...**A**δ **B**δ **C**δ...); the 9R stacking results when the oppositely signed dislocations separate. In contrast, the grain orientation of the{111}/{211} interface (which is approximately a Σ=99 orientation), is produced by Shockley partial dislocations distributed in a ratio n_{90}:n_{30}=2:1 (specifically ...**A**δ **A**δ **B**δ **A**δ **A**δ **C**δ...). As shown in Figure 3, separation of the positive 30° dislocations (**B**δ and **C**δ) from the negative 90° dislocations (**A**δ) transforms the right FCC crystal to the 9R stacking (*i.e*. ...abc/bca/cab...). Furthermore, the wall of 30° dislocations, acting as a low angle tilt boundary, would be expected to bend the planes in the dissociated region through an angle of 6.7°, which is consistent with the experimental observations.

Significance:

In developing a thorough understanding of interfaces, we would like to know what the basic functional units of a boundary are and how these relate to interfacial behavior. By successfully describing the decomposition mode and geometrical features of the {111}/{112} interface, our work points to the importance of Shockley partial dislocations as elements of interfacial structure and provides a key step in testing whether general high angle grain boundaries can be understood in terms of arrays of such defects.

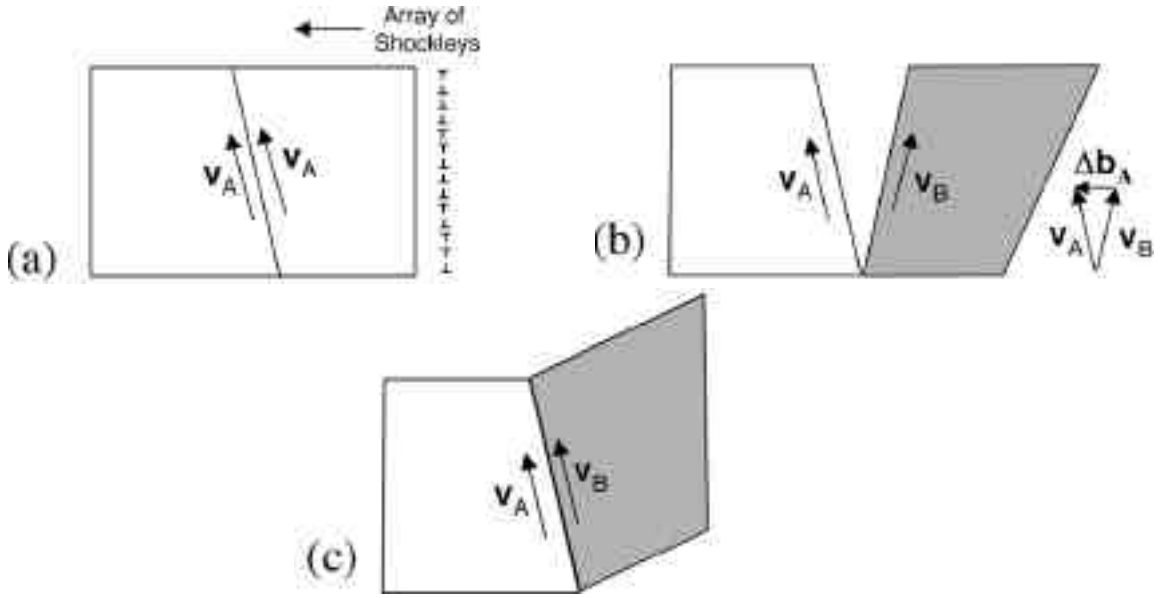

Figure 1. Schematic illustrating how grain orientation is partitioned into array of Shockley partial dislocations (SPDs). (a) Array of SPDs is swept into crystal up to the interface plane, indicated by $\mathbf{v_A}$. (b) This operation reorients the right crystal through a twinning operation. (c) The total orientation change is the combination of the twinning operation and the shape change due to the net Burgers vector, $\Delta\mathbf{b_A}$, of the array.

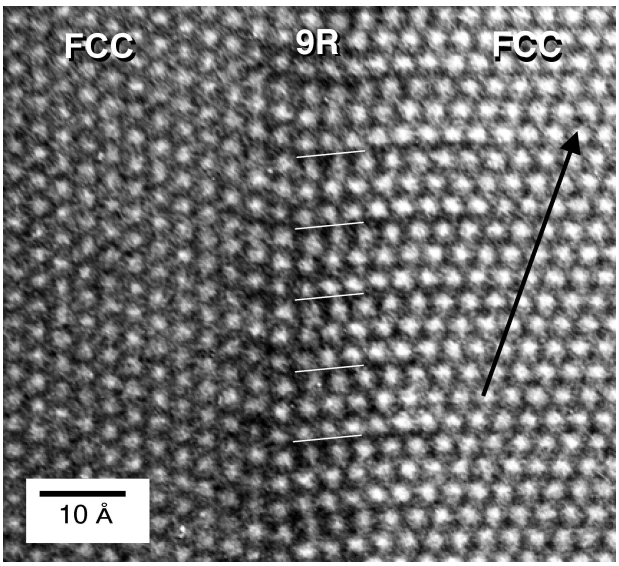

Figure 2. HRTEM image of {111}/{112} Au boundary. Note the 3-plane spacing and inclination of the stacking faults at the interface.

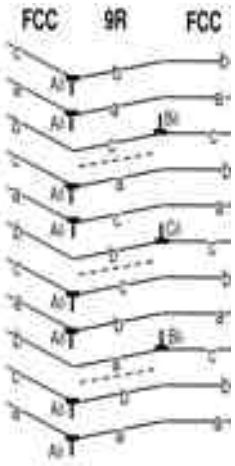

Figure 3. The fault distribution and plane bending occurs when the 30° (**B**δ**,** and **C**δ) and 90° Shockleys (**A**δ) that comprise this boundary separate.

Multi-Scale Modeling of Grain Boundary De-faceting Phase Transition

J.C Hamilton and I. Daruka

Publications:

Grain Boundary De-faceting, A First Order Phase Transition by Atomic Shuffle, I. Daruka and J. C. Hamilton, to be submitted.

Motivation:

Thermodynamic studies have predicted that phase transitions should occur at grain boundaries in solids. These predictions have been confirmed by hot-stage transmission electron microscope studies revealing a reversible de-faceting transition of Σ3{112} grain boundaries in Al at about 400K. In spite of its great practical and theoretical importance, the fundamental atomic processes involved in the de-faceting transition and the nature of the transition have not been resolved yet.

Accomplishment:

We have carried out EAM molecular dynamics (MD) simulations of the Σ3{112} grain boundaries in Al, using Voter-Chen aluminum potentials. At temperatures above 200K increasing disorder at the grain boundary facet junctions was observed with the grain boundary becoming smooth and diffuse at temperatures around and above 400K. This transition was reversible, the grain boundaries became faceted again upon cooling. We learned from these simulations that the grain boundary could move only by the collective motion of four atoms at the grain boundary junction (see insets of Fig. 1). This elementary excitation was mapped onto a simple two-dimensional lattice model incorporating both the geometry and the energy relations of the grain boundary. Extensive Monte-Carlo simulations were performed to investigate properties of the derived lattice model. In excellent agreement with the experiment and with the MD simulations, we found that at low temperatures the interface separating the two grains consists of faceted grain boundaries (Fig. 1a), while at high enough temperatures the facets disappear and the interface becomes rough at atomic length-scales (Fig. 1b). We showed that this de-faceting transition is a first-order phase transition in dramatic contrast to the continuous nature of surface roughening. Using the transfer-matrix method we were able to determine the phase transition temperature analytically.

Significance:

Our results, derived with the help of multi-scale modeling, provide a detailed understanding of the experimentally observed de-faceting phase transition of grain boundaries. The formulated lattice model also enables us to study other related phenomena, such as grain coarsening, and grain mobility in other thin film systems. The nature of the elementary excitation and the discontinuity of the de-faceting phase transition emphasize the difference between our model and other discrete models aimed to describe grain boundary melting or surface roughening.

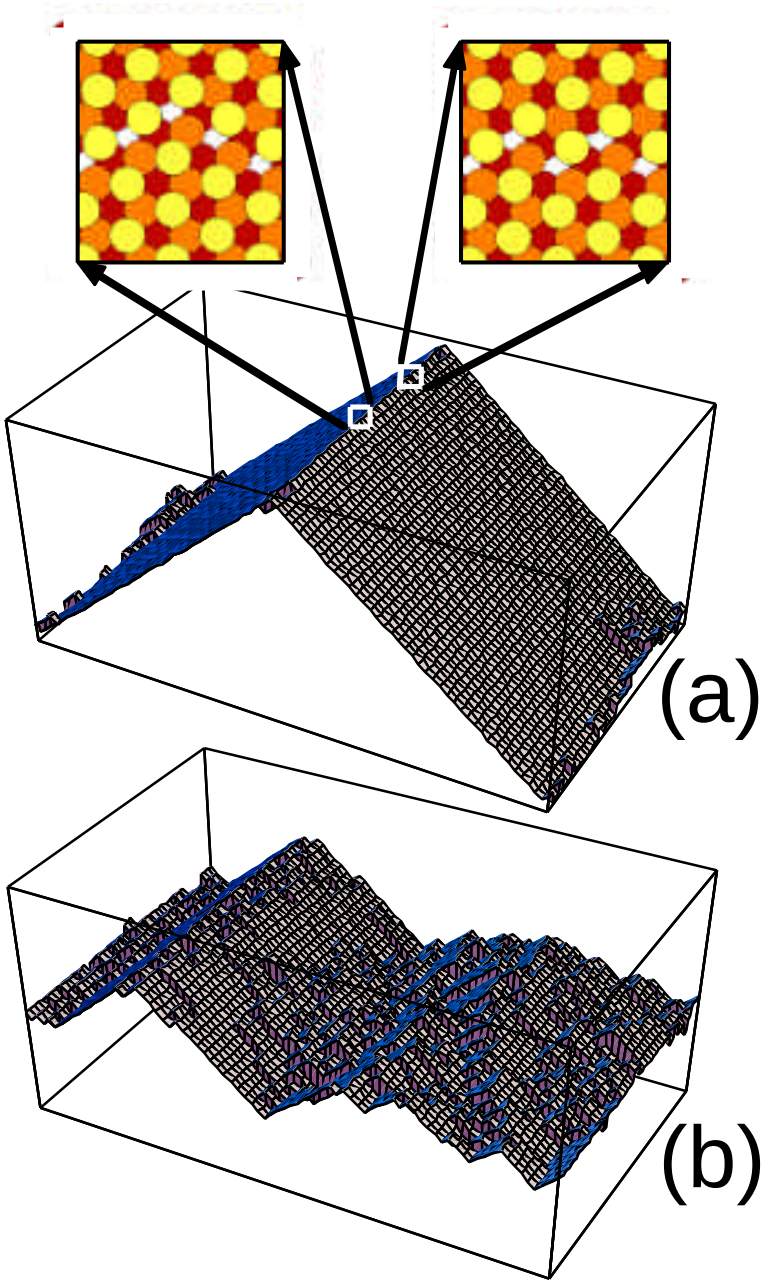

Fig. 1: Morphology of the Σ3{112} grain boundaries in Al: (a) well below the de-faceting transition temperature, (b) around the de-faceting temperature, obtained by MC simulations. The left inset shows the atomic structure at the junction of the two {112} grain boundary facets viewed along [111], calculated by embedded atom method simulations. The local rearrangement of atoms due to an elementary excitation at the junction is shown in the right inset. A movie of this de-faceting phase transition is included on the accompanying CDROM
(filename: **al grain boundary defaceting**) .

Morphological Evolution of Grain Boundary Facets

D.L. Medlin and G. Lucadamo

Publication:

"Morphological Evolution of a Fully Faceted Grain Boundary," D.L. Medlin and G. Lucadamo, in "Influences of Interface and Dislocation Behavior on Microstructure Evolution," eds. M. Aindow *et al.* (2001, MRS).

Motivation:

Grain boundaries are often faceted in extreme cases of interfacial anisotropy. Such a morphology prevents the application of classical notions of grain-boundary curvature to understanding microstructural evolution. Although there has been much effort at incorporating anisotropic grain-boundary properties, including faceted geometries, into computational approaches for microstructural evolution, at present our mechanistic understanding of the behavior of facets and their junctions remains limited.

Accomplishment:

We are conducting experiments to better understand the behavior of facets during grain evolution. Our initial focus is on the dynamics of Σ=3 $\{11\ \bar{2}\}$ facets in <111> oriented gold thin films. This system is ideally suited for these studies since the crystallography and structure of the boundaries is already well understood. An example of one such faceted grain is shown in Figure 1a to illustrate the fine-scale facet distribution typical of the initial, as-deposited films. As shown in Figure 1b, annealing dramatically increases the fraction of the boundary length composed of larger-scale facets. In order to determine the pathway by which this coarsening occurs, we are using *in situ* transmission electron microscopy to track the real-time evolution of the boundaries. The transition from an initial highly stepped boundary to a single corner is shown in the series of micrographs in Figure 2. From these observations, we have learned that the grain boundary facet coarsening is accompanied by the motion of perimeter conserving facets (*i.e.,* facets terminated by corners of opposite sense with respect to the Wulff surface).

Significance:

Our observations are surprising in light of the conventional view of grain-boundary facet evolution. Perimeter conserving facets have been thought to remain fixed until being passively consumed by facets terminated by corners of the same sense (which do not conserve the boundary perimeter and thus lead to a net reduction in interfacial energy). However, no explicit properties are assigned to the corners in such phenomenological constructions--junctions are treated simply as the geometric consequence of joining two facets. Thus an important question is raised: are there energetics associated with the junctions themselves that produce a driving force for facet motion? To address this question, we are currently measuring the short-time fluctuations in junction position to determine whether correlations exist that would be indicative of junction-junction interactions.

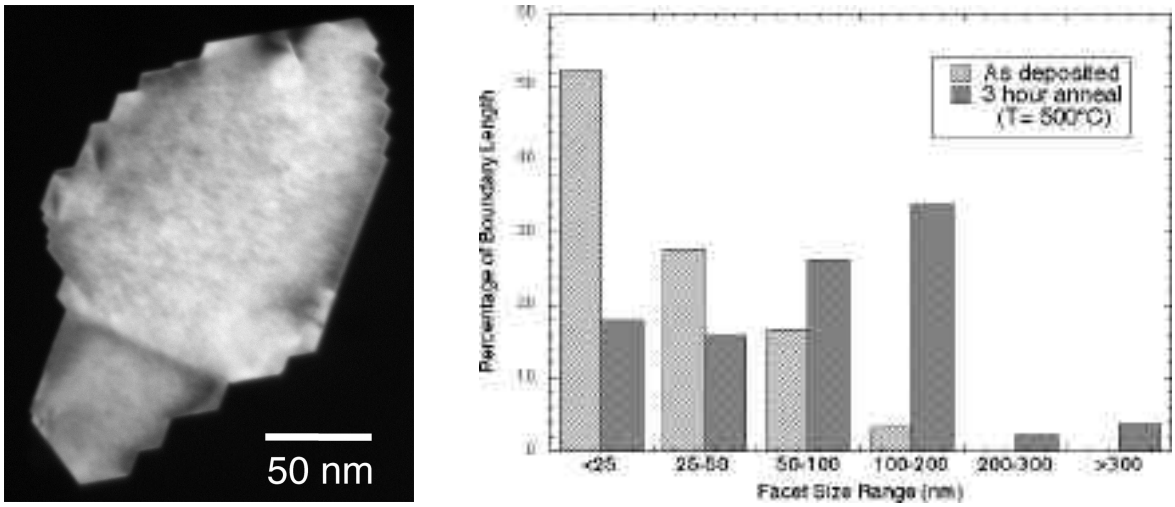

Figure 1. (a) Darkfield micrograph showing facet steps on an enclosed grain in an as-deposited Σ=3 Au film. (b) Graph shows the proportion of total grain-boundary length as distributed across the range of facet sizes for grains before and after annealing. Prior to annealing, the majority of facets are smaller than 50 nm. With annealing, an increased proportion of boundary length shifts to larger facet size.

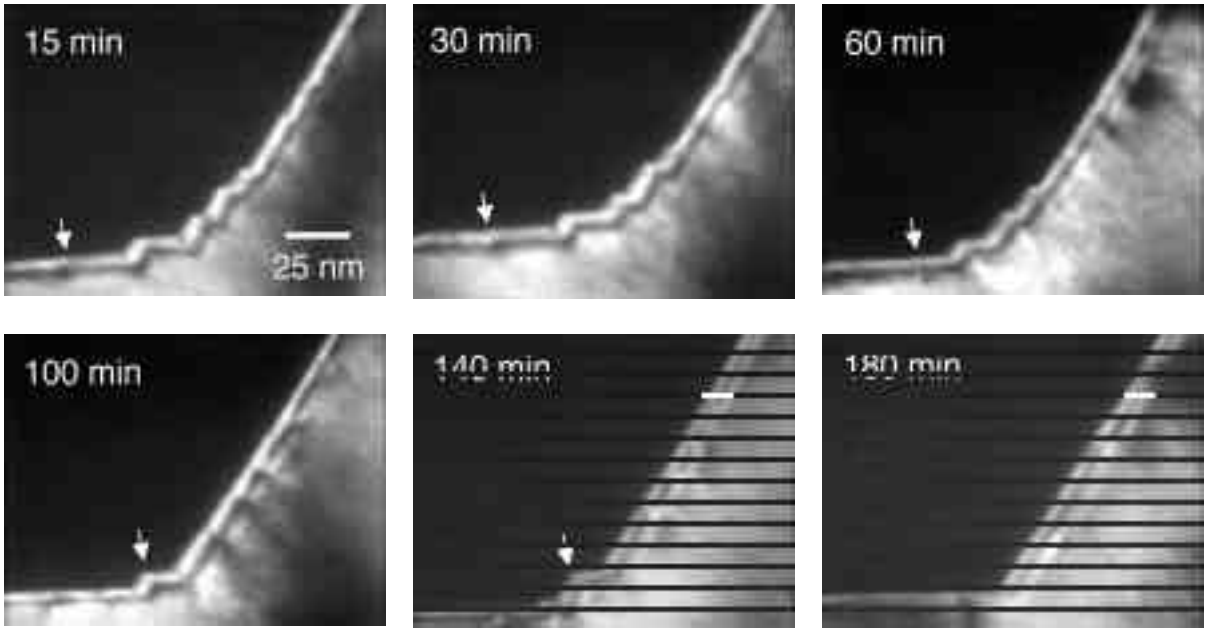

Figure 2. Stills taken from video showing motion of facets during evolution of boundary corner during annealing (T=490°C). The arrowed feature tracks a junction pair as it grows from a barely detectable feature in the initial stages to a well defined step (100 and 140 minutes) before shrinking again as the final corner develops. A movie showing this process is included on the accompanying CD-ROM (filename: **grain boundary facet evolution**).

Origin of Dislocations at Grain Boundary Facet Junctions

G. Lucadamo and D.L. Medlin

Publication:

"Dislocation Emission at Junctions between Σ=3 Grain Boundaries in Gold Thin Films" G. Lucadamo and D.L. Medlin, submitted to *Acta materialia*.

Motivation:

Dislocation arrays that appear to emanate from grain boundary junctions are commonly observed in thin films. Since such dislocations can play important roles in both the microstructural evolution and strain response of a thin film, it of interest to determine their origin and relationship to grain boundaries.

Accomplishment:

In this study, we have investigated the behavior of dislocations at grain boundary facet junctions in [111] oriented Au Σ=3 bicrystal films. This system was chosen because the interfacial crystallography and structure are already well understood and because interfaces can be produced straightforwardly via epitaxial growth techniques. Although the boundaries in this system consist largely of {112} facets that run through the thickness of the film, in some cases the boundary is jogged producing a horizontal {111} boundary (see Figure 1). At such junctions, we frequently find parallel arrays of 1/6<112> dislocations lying on the horizontal {111} twin. Through diffraction contrast analysis and *in situ* TEM measurements (Figure 1), we have determined that these defects originate from arrays of secondary grain boundary dislocations on the {112} facets ahead of the junction. At elevated temperatures, the dislocations move by climb until reaching the junction. To move past the junction an additional dislocation segment, which moves by glide, must be created on the {111} twin. This phenomenon was surprising to us since the formation of additional dislocation line length would seem to increase the energy of the system. However, a calculation of the strain energy of this configuration shows that the elastic repulsion of the dislocations is sufficient to dominate the increase in dislocation line energy for dimensions and dislocation arrays sizes comparable to what we have observed.

Significance:

These results show a simple process by which grain boundary dislocations can be transformed to a glissile configuration at a twin boundary. Although we have considered only the specific case of a bicrystal facet junction, it is conceivable that similar processes can occur more generally at the intersection of twin boundaries with triple junctions. Thus, this work identifies a strain relief mechanism that should be considered in analyses of thin film plasticity in polycrystalline materials.

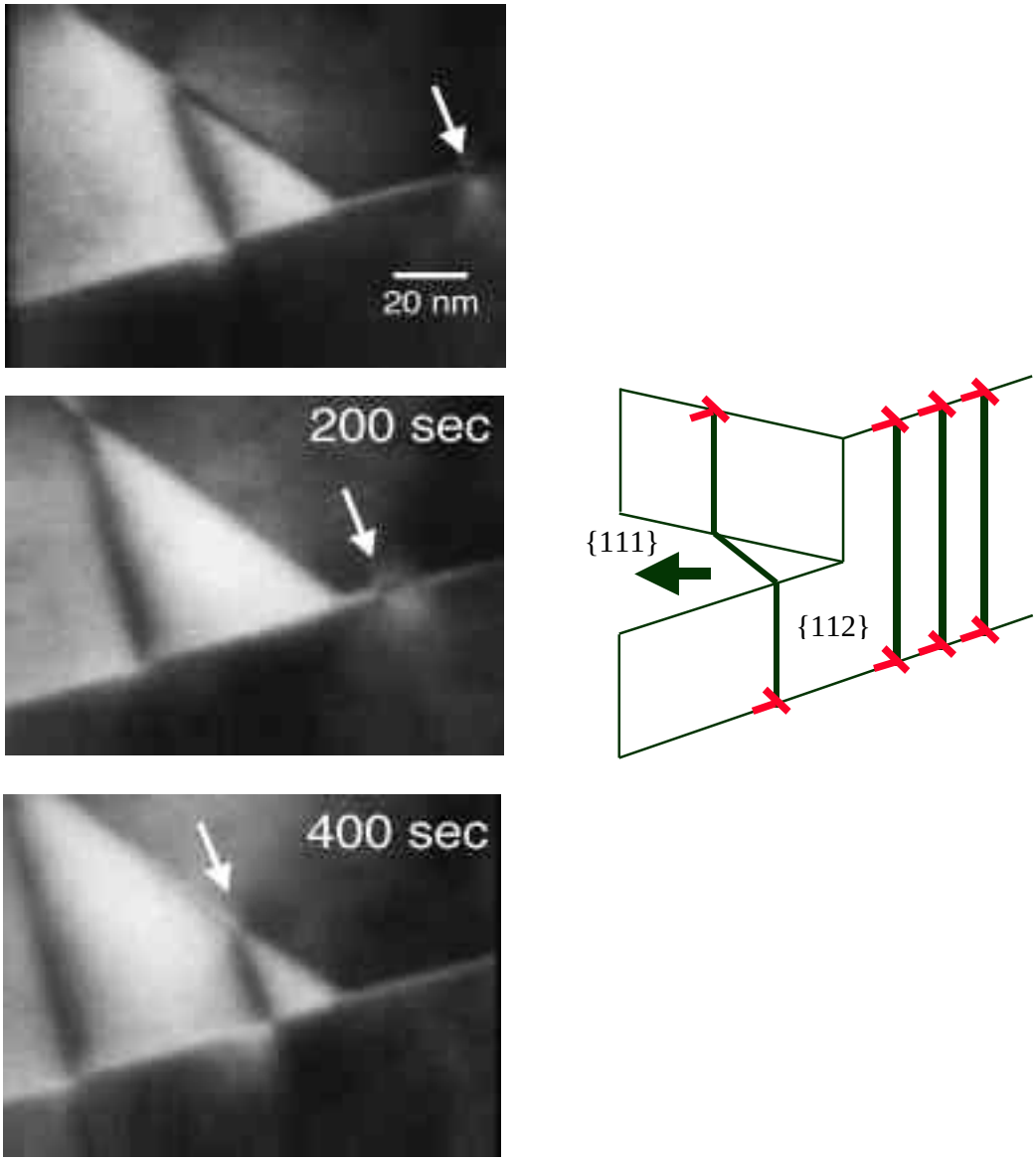

Figure 1. Sequence of stills taken from *in situ* TEM study showing the motion of dislocations on a {111} twin in gold. T=550°C. The arrow marks the position of a secondary grain boundary dislocation that initially lies on the {112} facet ahead of the junction. As illustrated in the schematic, as the dislocations climb past the facet junction they must create an additional length of dislocation line on the horizontal {111} facet. A movie showing the motion of these dislocations is included on the accompanying CD-ROM (filename: **dislocation emission**)

Atomistic Models of Dislocation Nucleation during Nanoindentation

C.L. Kelchner and J.C. Hamilton

Publications:

"Dislocation Nucleation and Defect Structure During Surface," C. L. Kelchner, S. J. Plimpton, and J. C. Hamilton, Physical Review **B 58**, 11085 (1998).

Motivation:

The continuing drive to reduce the size of electrical and mechanical devices is forcing materials science into domains where conventional ideas must be subject to careful scrutiny. At short length scales, atomistic effects must be added to continuum analysis. One of the classic tests for materials properties is indentation. Smaller and smaller "indenters" have been developed including the nanoindenter, the atomic force microscope, and the interfacial force microscope. Recent observations have shown that ideas regarding plastic thresholds which were developed for macroscopic indenters are not reliable at the spatial scale of some of the new instruments. The present theoretical work aims to understand dislocation nucleation under indentation at these spatial scales. Exactly where and how the initial dislocations form has been largely a matter of speculation. We have performed atomistic calculations of the nucleation of dislocations during indentation to resolve this issue.

Accomplishment:

We have modeled indentation by combining a frictionless indenter with atomistic calculations. In order to study the defect structure of the indented surface in detail, the location and type of defects present must be reliably identified and separated from the extensive elastic deformation in the system. We have developed a general solution to this problem for a centrosymmetric material which relies on the fact that homogeneous elastic deformation does not break centrosymmetry. This solves a long standing problem in the imaging and interpretation of atomistic calculations of dislocation structures. The system chosen for study was a Au(111) surface. Our calculations show that the dislocations nucleate on the {111} glide planes just below the surface then grow into the bulk lattice. A snapshot of the system near the beginning of this nucleation process is presented in Figure 1, with stacking faults shown as dark gray and partial dislocations as light gray (surface atoms are also shown in white). The structure formed after these initial dislocations finish growing is shown in Figure 2.

Significance:

This work provides the first atomistic imaging of dislocation nucleation during indentation of a passivated surface. Although the maximum shear stress from continuum theory is centered underneath the indenter at a depth of about half the contact radius, our results clearly show that this is not where the dislocations nucleate. This implies that the commonly used criterion for plastic yield in a material, i.e., that the maximum shear stress under the indenter exceed the theoretical shear stress of the material, is at best a crude approximation. In addition, these atomistic calculations provide the complex asymmetric defect structure that results from the initial dislocations and which had been previously unavailable. We believe that the dislocation imaging technique developed here is superior to any existing technique and will find wide applicability in theoretical modeling of defect structures in centrosymmetric materials.

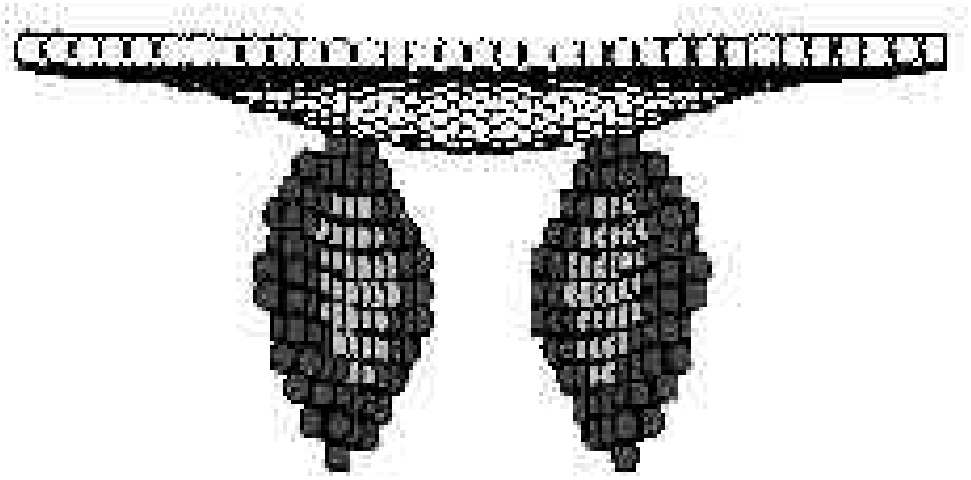

Figure 1. Snapshot of the initial stage of dislocation nucleation during indentation of Au(111). The shading indicates defect types: partial dislocation (dark gray), stacking fault (light gray), and surface atoms (white). The atoms in regions having only elastic strain are not shown. The surface deformation is due to the indenter pressing into the surface. A movie of the nucleation process is included on the accompanying CDROM.
(Filename: **au111 indentation nucleation**)

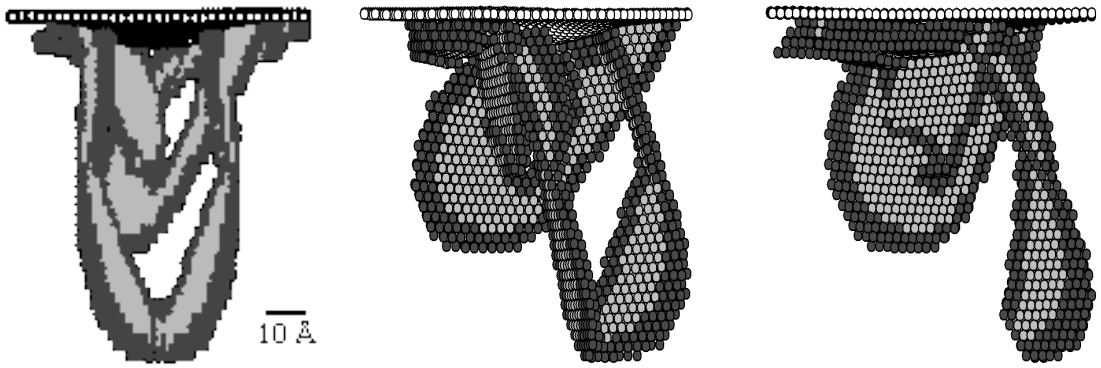

Figure 2. Equilibrium defect structure at the onset of plastic deformation during indentation of Au(111), (a) view along $[11\bar{2}]$, (b) rotated 45˚ about [111], and (c) rotated 90˚ to $[1\bar{1}0]$. The shading indicates defect types as in Figure 1. The viewing direction is identical in Figure 2(a) and in Figure 1. A movie showing a 3-D rotation of this structure is included on the accompanying CDROM. (Filename: **au111 indentation rotation**)

FUTURE WORK

Over the next three years we plan to build on our work investigating the structure and dynamic behavior of grain boundaries. A longstanding issue has been to understand how dislocations, which we understand very well in the bulk, are related to the elements of grain boundary structure, particularly at high angle boundaries. Such an understanding is vital, for instance, to elucidating the details by which bulk lattice dislocations interact with grain boundaries or recombine to form new boundary structures. Our work so far has made progress in highlighting the role of Shockley partial dislocations as elements of boundary structure. The question is whether this approach can be further generalized. We plan next to investigate whether this description can be extended by introducing additional dislocation arrays. As a starting point, we will investigate defect structures in symmetric FCC <110> tilt boundaries with misorientations near 38.9° (Σ=9 {141}) (e.g. see Figure 1) and 141° (Σ=9 {212}). Our observations are being conducted on boundaries in gold, produced through an epitaxial growth technique, and in aluminum, using melt-grown bicrystals fabricated as part of a collaboration with Prof. C.L. Briant, Brown University. These boundaries are important test cases since, as illustrated in Figure 2, they fall outside the range of <110> tilt boundaries, specifically 50.5° (Σ=11 {131}) to 109.5° (Σ=3 {111}), that can be described with a single array of Shockley partial dislocations [36]. Furthermore, the Σ=9 {141} boundary has particular significance within the well-known "Structural Unit Model" of Sutton and Vitek [50] because it is expected to be composed of equal contributions of the fundamental units found in the nearby 31.6° (Σ=27 {151}) and 50.5° (Σ=11 {131}) boundaries. However, recently there has been some question as to whether the Structural Unit Model is applicable to boundaries that dissociate into three dimensional configurations[33]. From our analysis of the dislocation structure of these boundaries we hope to find a route to unifying these different models of boundary structure.

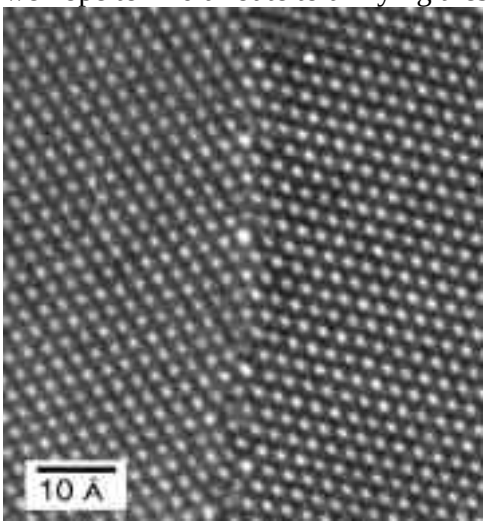

Figure 1. HRTEM image of aluminum grain boundary near the 38.9° Σ=9 {141} orientation.

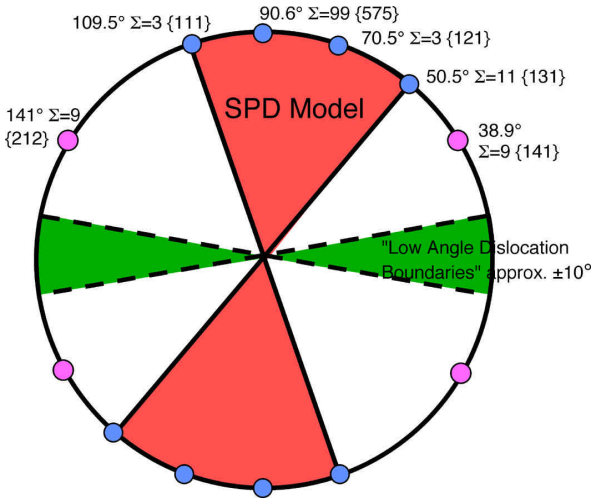

Figure 2. Schematic showing range of symmetric <110> boundary orientations that can be described by a single Shockley partial dislocation (SPD) array.

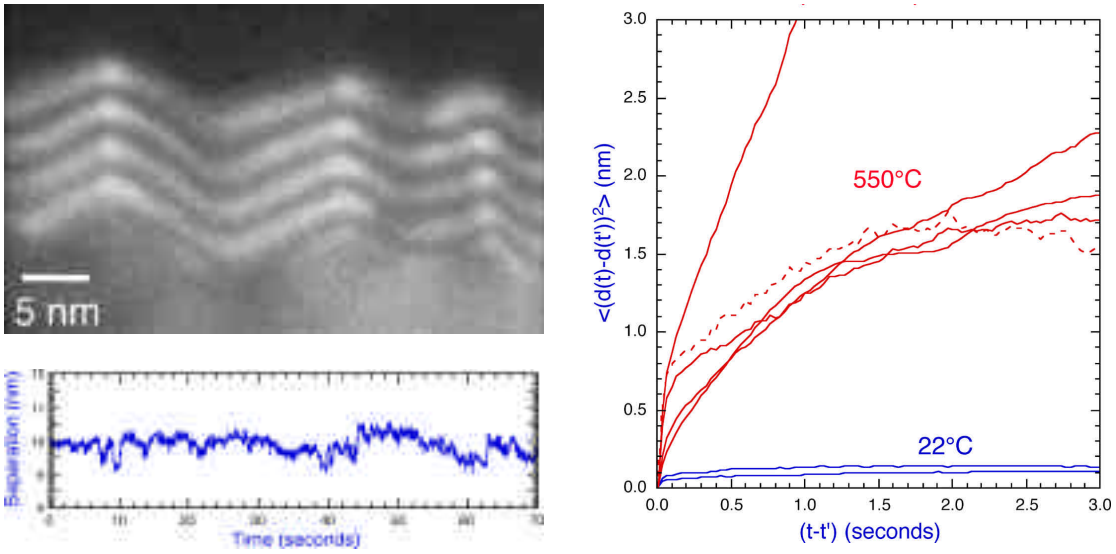

Figure 3. The left plot shows an example of the thermal fluctuations in junction separation measured from *in situ* TEM observations (550°C) of Σ=3 {112} boundaries in Au. Autocorrelation analysis of such data allows us to characterize the statistical behavior of the fluctuations, as shown on the right. The deviation from linearity in these plots of the mean-squared-displacements indicates a departure from a pure random walk.

In our studies of grain boundary dynamics we are now focussing on the behavior of boundary junctions. An important issue is to determine the forces associated with such junctions, and what influences these have on the dynamical behavior of a boundary. We are currently addressing this question by quantifying the thermal fluctuations of junctions that separate {112} facets in Σ=3 gold films (see Figure 3). By measuring the temporal correlations in the junction motion, we hope to probe the degree of interaction between adjacent junctions using the technique of Bartelt *et al.* [51]. These interactions are central to determining the dynamical evolution of faceted interfaces. Additionally, we plan to begin an investigation of the processes that occur during the impingement of two boundaries to form triple-, and higher-order, junctions. To directly observe the atomic-level dynamical processes, we will utilize the new *in situ* HRTEM facility at the National Center for Electron Microscopy (LBL) in collaboration with E. Stach. We will begin by studying the boundary collision processes in multiply-twinned <110> oriented Au films that form boundaries in the Σ=9 orientation. Thus, this work will directly complement our upcoming structural studies and will provide an experimental vehicle for testing the dynamical implications of the dislocation-based models of boundary structure.

A new area, which we intend to address, is the role of impurities on grain boundary properties. This is a challenging endeavor because computationally fast methods such as the embedded atom method cannot handle typical interstitial impurties. Consequently computationally intensive first principles methods will be essential for this important class of problems. It is well known that impurities segregate to grain boundaries changing the properties of bulk metals. Sulfur embrittlement of steel is an example of this phenomena. Recent experiments demonstrate that impurities in aluminum change the rate of grain boundary motion dramatically[52, 53]. The mechanisms underpinning these phenomena are not well understood, although significant progress is being made using Monte-Carlo simulations and postulating

interactions between the grain boundary and impurities[54]. We intend to apply the increasing power of first principles atomistic calculations to quantify the interactions between impurities and grain boundaries. Initially, we will determine favored sites for carbon at a Σ=3 {112} grain boundary in nickel. This is a boundary we already understand well from previous structural studies. We will also determine the activation energies required to diffuse carbon in the vicinity of this boundary. Finally, we will investigate the effect of carbon on activation energies for processes such as grain boundary sliding and fracture.

DESCRIPTION OF MOVIE FILES

Grain Boundary De-faceting
(Filename: al grain boundary defaceting)
This movie shows a Monte-Carlo simulation of grain boundary de-faceting at an aluminum twin boundary with average $[01\bar{1}]$ orientation. The temperature is cycled from 500K to 600K in a linear ramp and then back down to 500K. Initially the grain boundary is faceted into two {112} type facets. There is a small amount of disorder near the facet junctions. As the temperature rises, large fluctuations are seen near the phase transition temperature. Above the transition temperature the grain boundary is approximately flat with the average $[01\bar{1}]$ orientation. As the temperature is decreased the process is reversed and the grain boundary facets.

Grain Boundary Sliding
(Filename: al grain boundary shearing)
This movie shows grain boundary sliding at an aluminum $[11\bar{2}]$ twin boundary. The atomic planes are colored to facilitate identification of atoms and atomic planes. As the grain boundary slides with the right hand grain moving up, the grain boundary migrates to the left. This coupling of grain boundary sliding with grain boundary migration has been seen in many experimental studies. At an atomic level, the transfer of atoms from one side of the grain boundary to the other is required for the boundary to migrate. This transfer is caused by steric hindrance of atomic pairs at the grain boundary. This steric hindrance prohibits the two halves of the bicrystal from moving rigidly past each other without transfering atoms.

Dislocation Nucleation during Surface Indentation
(Filename: au111 indentation nucleation)
This movie shows dislocation nucleation in the near surface region during surface indentation of a gold (111) surface. The white atoms at the top represent the surface with a spherical depression caused by the indenter. The red atoms represent partial dislocations which nucleate and then grow into two partial dislocation loops under the indenter. The yellow atoms represent stacking faults which are surrounded by the dislocation loops. Eventually the dislocation loops grow to a point where they interact and then merge.

Dislocation Structure after Surface Indentation
(Filename: au111 indentation rotation)
This movie shows the final structure after the first plastic yield point for surface indentation of a gold (111) surface. The movie shows the rotation of this dislocation structure about the surface normal. The white atoms represent the surface, the red atoms represent partial dislocations, and the yellow atoms represent stacking faults. The structure is rotated about the indenter axis in order to show the three-dimensional dislocation structure under the indenter.

Grain Boundary Facet Evolution
(Filename: grain boundary facet evolution)
This is a time-lapse movie showing *in situ* TEM observations of the morphological evolution of a faceted Σ=3 boundary in a gold thin film over a three-hour time period. Since the images were

obtained in a darkfield condition, the upper grain, which is out of the strong diffracting condition, appears black. The temperature is 490°C and the horizontal field of view is 150 nm.

Dislocation Emission at Grain Boundary Facet Junction
(Filename: dislocation emission)
This is a movie showing *in situ* TEM observations of the motion of dislocations in a gold thin film at the junction of a {111} twin with two {112} facets over a 400 second time period. A secondary grain boundary dislocation that initially lies on the {112} facet, ahead of the junction, climbs past the junction, creating additional length of dislocation line on the horizontal {111} facet. The temperature is 550°C and the horizontal field of view is 130 nm.

REFERENCES

1 A. P. Sutton and R. W. Balluffi, *Interfaces in Crystalline Materials* (Clarendon Press, Oxford, 1995).

2 G. Gottstein and L. Shvindlerman, *Grain Boundary Migration in Metals* (CRC Press, Boca Raton, 1999).

3 M. J. Mills, M. S. Daw, G. J. Thomas, et al., Ultramicroscopy **40**, 247 (1992).

4 D. L. Medlin, M. J. Mills, W. M. Stobbs, et al., in *Atomic-Scale Imaging of Surfaces and Interfaces* (MRS, Pittsburgh, 1993), Vol. 295, p. 91.

5 U. Dahmen, C. J. D. Hetherington, M. A. O'Keefe, et al., Phil. Mag. Letters **62**, 327 (1990).

6 G. H. Campbell, S. M. Foiles, P. Gumbsch, et al., Phys. Review Letters **70**, 449 (1993).

7 D. Hofmann and F. Ernst, Ultramicroscopy **53**, 205 (1994).

8 A. H. King and D. A. Smith, Acta Cryst. **A36**, 335 (1980).

9 R. C. Pond, in *Dislocations in Solids*, edited by F. R. N. Nabarro (Elsevier Science Publishers, 1989), p. 1.

10 J. P. Hirth and R. C. Pond, Acta materialia **44**, 4749 (1996).

11 J. W. Cahn and G. Kalonji, Journal of Physics and Chemistry of Solids **55**, 1017 (1994).

12 G. P. Dimitrakopulos, T. Karakostas, and R. C. Pond, Interface Science **4**, 129 (1996).

13 A. H. King, Interface Science **7**, 251 (1999).

14 M. S. Daw, S. M. Foiles, and M. I. Baskes, Materials Science Reports **9**, 251 (1993).

15 Jónsson, G. Mills, and K. W. Jacobsen, in *Classical and Quantum Dynamics in condensed Phase Simulations*, edited by B. J. Berne, G. Ciccotti and D. F. Coker (World Scientific, Singapore, 1998).

16 D. Vanderbilt, Phys. Rev. B **41**, 7892 (1990).

17 G. Kresse and J. Furthmuller, Physical Review B **54**, 11169 (1996).

18 J. C. Hamilton and S. M. Foiles, submitted to Physical Review B, (2001).

19 O. N. Mryasov, Y. N. Gornostyrev, and A. J. Freeman, see LANL cond-mat/0006257 (unpublished), (2000).

20 O. Mryasov, Y. N. Gornosryev, M. v. Schilfgaarde, et al., Materials Science and Engineering A **309**, 310 (2001).

21 J. Hamilton and S. M. Foiles, Physical Review Letters **75**, 882 (1995).

22 R. Peierls, Proc. Phys. Soc. London **52**, 34 (1940).

23 V. Vitek, Cryst. Latt. Def. **5**, 1 (1974).

24 M. Methfessel, M. vanSchilfgaarde, and R. A. Casali, in *Electronic Structure and Physical Properties of Solids: The Uses of the LMTO Method*, edited by H. Dreysse (Springer-Verlag, Berlin, 2000).

25 D. L. Medlin, in *Advances in Twinning*, edited by S. Ankem and C. S. Pande (TMS, Warrendale, Pennsylvania, 1999), p. 29.

26 S. M. Foiles and D. L. Medlin, Materials Science and Engineering A (accepted for publication), (2001).

27 D. Roundy, C. R. Krenn, M. L. Cohen, et al., Physical Review Letters **82**, 6999 (1999).

28 D. L. Medlin, G. H. Campbell, and C. B. Carter, Acta Materialia **46**, 5135 (1998).

29 D. L. Medlin, S. M. Foiles, G. H. Campbell, et al., Materials Science Forum **294-298**, 35 (1999).
30 W. Krakow and D. A. Smith, Ultramicroscopy **22**, 47 (1987).
31 K. L. Merkle, Colloque de Physique C1 **51**, C1:251 (1990).
32 K. L. Merkle, J. Phys. Chem. Solids **55**, 991 (1994).
33 J. D. Rittner and D. N. Seidman, Physical Review B **54**, 6999 (1996).
34 F. Ernst, M. W. Finnis, D. Hofmann, et al., Physical Review Letters **69**, 620 (1992).
35 U. Wolf, F. Ernst, T. Muschik, et al., Philosophical Magazine A **66**, 991 (1992).
36 D. L. Medlin, S. M. Foiles, and D. Cohen, Acta Materialia **49**, 3687 (2001).
37 I. Daruka and J. C. Hamilton, to be submitted, (2001).
38 J. W. Cahn, Journal de Physique **43**, 199 (1982).
39 T. E. Hseih and R. W. Balluffi, Acta metallurgica **37**, 2133 (1989).
40 D. L. Medlin and G. Lucadamo, in *Influences of Interface and Dislocation Behavior on Microstructure Evolution*, edited by M. A. e. al. (Materials Research Society, Pittsburgh, 2001), Vol. 652, p. Y3.4.1.
41 J. E. Taylor, J. W. Cahn, and C. A. Handwerker, Acta Metall. Mater. **40**, 1443 (1992).
42 G. Lucadamo and D. L. Medlin, submitted to Acta materialia, (2001).
43 E. A. Stach, U. Dahmen, and W. D. Nix, in *Recent Developments in Oxide and Metal Epitaxy-Theory and Experiment*, edited by M. Y. e. al. (Materials Research Society, Pittsburgh, 2000), Vol. 619, p. 27.
44 K. Owusu-Boahen and A. H. King, Acta Materialia **49**, 237 (2001).
45 T. J. Balk, G. Dehm, and E. Arzt, in *Dislocations and Deformation Mechanisms in Thin Films and Small Structures*, edited by K. S. e. al. (Materials Research Society, Pittsburgh, 2001), Vol. 673, p. P2.7.1.
46 C. L. Kelchner, S. J. Plimpton, and J. C. Hamilton, Physical Review B **58**, 11085 (1998).
47 J. D. Kiely, R. Q. Hwang, and J. E. Houston, Physical Review Letters **81**, 4424 (1998).
48 J. A. Zimmerman, C. L. Kelchner, P. A. Klein, et al., Physical Review Letters **(accepted for publication. To appear October 15,2001)** (2001).
49 O. R. delaFuente, J. A. Zimmerman, M. A. Gonzalez, et al., submitted to Physical Review Letters, (2001).
50 A. P. Sutton and V. Vitek, Phil. Trans. Royal Society London A **309**, 1 (1983).
51 N. C. Bartelt, T. L. Einstein, and E. D. Williams, Surface Science **240**, L591 (1990).
52 G. Gottstein, D. A. Molodov, and L. S. Shvindlerman, Interface Science **6**, 7 (1998).
53 D. A. Molodov, U. Czubayko, G. Gottstein, et al., Acta Materialia **46**, 553 (1998).
54 M. I. Mendelev and D. J. Srolovitz, Acta Materialia **49**, 2843 (2001).